J. of Supercritical Fluids 95 (2014) 394–406

Contents lists available at ScienceDirect

The Journal of Supercritical Fluids

journal homepage: www.elsevier.com/locate/supflu

The effect of ethyl-lactate and ethyl-acetate plasticizers on PCL and PCL–HA composites foamed with supercritical CO_2

A. Salerno [a], M.A. Fanovich [b,*], C. Domingo Pascual [a]

[a] Institut de Ciència de Materials de Barcelona (ICMAB), Campus de la UAB, Barcelona, Spain
[b] Instituto de Investigaciones en Ciencia y Tecnología de Materiales (INTEMA), Av. Juan B. Justo 4302, B7608FDQ Mar del Plata, Argentina

ARTICLE INFO

Article history:
Received 16 August 2014
Received in revised form 8 October 2014
Accepted 9 October 2014
Available online 22 October 2014

Keywords:
Foaming
Hydroxyapatite
Plasticizer
Polycaprolactone
Scaffold
Supercritical CO_2

ABSTRACT

The present study reports foaming of polycaprolactone (PCL) and PCL nano- and micro-composites with dispersed hydroxyapatite (HA) particles by means of binary mixtures of supercritical CO_2 ($scCO_2$) and either ethyl lactate (EL) or ethyl acetate (EA) as plasticizer. The effect of the size and concentration of HA particles, as well as the effects of the plasticizer type and the incorporation route were investigated aiming to fabricate porous scaffolds with uniform morphology and controlled pore size distribution. For this purpose, foaming experiments were carried out by selecting two operating temperatures, 40 and 45 °C, and two soaking times, 1 and 17 h. Furthermore, a double step of depressurization was used to promote the development of a double-scale pore size structure in porous scaffolds useful for tissue engineering.

The results of this study indicated that supercritical foaming of PCL and PCL–HA composites is enhanced when the selected operating temperature and time are 45 °C and 17 h, respectively. Furthermore, although both EL and EA plasticizers enhanced the low temperature foaming of the materials, we demonstrated that the route of incorporation of the plasticizer is a critical aspect for enhancing composite foaming and scaffold fabrication. From this point of view, the best results were achieved when EA was pre-mixed with the polymeric powder for preparing a dough for the foaming process.

1. Introduction

The development of bone graft substitute materials has promoted new designs that aim to optimize the composition, microstructure and biological properties thereof. In particular, materials used for bone tissue regeneration have wide ranges of composition, spanning from bioactive glass materials to biodegradable polymers, as well as their composites [1]. This is because for bone tissue regeneration it is essential that the material presents bioactivity which depends on its composition and nano- and micro-structure. In this field, specific calcium phosphates, such as hydroxyapatite (HA, $Ca_{10}(PO_4)_6(OH)_2$)-based materials, are the protagonists. Indeed, these materials have a chemical composition that mimics the natural mineral phase of bone tissue, thus providing a bioactive behaviour for osseointegration, degradation and remodelling thereof. However, the difficulties associated with the fragile nature of the calcium phosphate materials have promoted the development of composite materials of calcium phosphates dispersed in a polymer matrix with adequate microstructures and sufficient mechanical strength [2,3]. Among the different polymer-composite combinations available, the most interesting and successful for the preparation of porous substrates useful in bone regeneration employs a polycaprolactone (PCL) matrix and hydroxyapatite (HA) filler. Depending on the size of the HA particles, the final product is either nano or microstructured. It is possible to process these hybrid composites with the required porosity through a foaming technique [4–7].

Gas foaming of polymers or composites including biodegradable/biocompatible polymers by using supercritical CO_2 as blowing agent is a widely accepted method. CO_2 allows to work in a clean and safe environment. Moreover, the establishment of a narrow pore size distribution, easy solvent recovery, good plasticizing ability and high diffusivity of the gas are all advantages of using supercritical CO_2 ($scCO_2$) in foaming processes [8]. Various porous PCL-based materials and composites foams have been produced by using $scCO_2$ foaming [9–13]. In a typical process, the polymer is exposed to CO_2 at saturation pressure and

* Corresponding author. Tel.: +54 223 481 6600; fax: +54 223 481 0046.
E-mail addresses: mafanovi@hotmail.com, mafanovi@fi.mdp.edu.ar (M.A. Fanovich).

http://dx.doi.org/10.1016/j.supflu.2014.10.007
0896-8446/

Table 1
Processing conditions used during foaming experiments.

Test	Sample composition	Blowing agent	Sample preparation	Saturation time [h]	Temperature [°C]	Pressure [MPa]
1	PCL PCL–mHA5, PCL–mHA10 PCL–nHA5, PCL–nHA10	CO_2	Compacted powder	1	40	20
2	PCL PCL–mHA5, PCL–mHA10 PCL–nHA5, PCL–nHA10	CO_2	Compacted powder	1	45	20
3	PCL PCL–mHA5, PCL–mHA10 PCL–nHA5, PCL–nHA10	CO_2 + EL	Compacted powder	1	40	20
4	PCL PCL–mHA5, PCL–mHA10 PCL–nHA5, PCL–nHA10	CO_2 + EL	Compacted powder	1	45	20
5	PCL PCL–mHA5, PCL–mHA10 PCL–nHA5, PCL–nHA10	CO_2	Compacted dough (EA + powder)	1	40	20
6	PCL PCL–mHA5, PCL–mHA10 PCL–nHA5, PCL–nHA10	CO_2	Compacted dough (EA + powder)	1	45	20
7	PCL PCL–mHA5, PCL–mHA10 PCL–nHA5, PCL–nHA10	CO_2	Compacted dough (EL + powder)	1	40	20
8	PCL PCL–mHA5, PCL–mHA10 PCL–nHA5, PCL–nHA10	CO_2	Compacted dough (EL + powder)	1	45	20
9	PCL PCL–mHA5, PCL–mHA10 PCL–nHA5, PCL–nHA10	CO_2	Compacted powder	17	45	20
10	PCL PCL–mHA5, PCL–mHA10 PCL–nHA5, PCL–nHA10	CO_2 + EL	Compacted powder	17	45	20
11	PCL PCL–mHA5, PCL–mHA10 PCL–nHA5, PCL–nHA10	CO_2 + EA	Compacted powder	17	45	20
12	PCL PCL–mHA5, PCL–mHA10 PCL–nHA5, PCL–nHA10	CO_2	Compacted dough (EL + powder)	17	45	20
13	PCL PCL–mHA5, PCL–mHA10 PCL–nHA5, PCL–nHA10	CO_2	Compacted dough (EA + powder)	17	45	20

temperature (higher than the critical point of CO_2), which reduces the apparent glass transition temperature or melting point to the processing temperature (plasticization) [14]. After venting the CO_2 by depressurization, the thermodynamic instability causes supersaturation of the CO_2 dissolved in the polymeric matrix and hence, nucleation of pores occurs. The growth of the pores continues until the polymer vitrifies. The saturation pressure, the saturation temperature and the depressurization profile are the critical parameters in determining the number of pores and the pore size distribution.

There are many reported studies on foaming of polymeric materials by using $scCO_2$. However, the studies related to $scCO_2$ foaming of nano and micro composites composed of HA particles in a PCL matrix are very limited. Recently, Salerno et al. [11] reported the preparation of porous PCL- 5%HA scaffolds with a bi-modal pore size distribution and highly interconnected pores, obtained by applying a two-step depressurization process. Markočič et al. [15] have determined the solubility and diffusivity of CO_2 in heterogeneous systems (PLLA-HA and PLGA-HA composites) that showed high values of both parameters influenced by the pressure and the

Table 2
DSC results of the PCL and PCL–HA composite samples before and after foaming.

Sample		T_M [°C]	T_i–T_f [°C]	Crystallinity [%]
Non foamed	PCL	59.5	37–69	72
	PCL–mHA5	60.9	44–68	75
	PCL–mHA10	61.2	47–67	75
	PCL–nHA5	60.8	46–67	75
	PCL–nHA10	60.0	46–66	75
Foamed	PCL (test #1)	59.3	26–69	57
	PCL (test #2)	60.6	30–70	52
	PCL (test #9)	58.5	29–63	52
	PCL (test #13)	59.1	26–66	52

content of the ceramic filler. In these systems, the presence of the HA particles acts as an obstruction for CO_2 diffusivity, thus, hindering the diffusion of gas into the composite. On the other hand, Tsivintzelis et al. [16] showed that more uniform pore structures were produced when CO_2-ethanol supercritical mixtures were used as blowing agents instead of pure CO_2. The authors concluded that small amounts of organic solvents can be used to overcome the difficulties related to the foaming of PCL materials, being the concentration of the organic solvent a new key parameter of the process. However, the use of plasticizers with $scCO_2$ to facilitate the processing of composites involving inorganic fillers is not sufficiently explored.

This work reports a systematic and exhaustive study of foaming of nano and microstructured composites of PCL and HA (5, 10 wt%) by using $scCO_2$ in combination with two recognized safe organic solvents, ethyl lactate (EL) and ethyl acetate (EA). Two routes of incorporation of these plasticizers are reported. The optimization of the morphological and structural characteristics of the prepared scaffolds is achieved by the control of the foaming parameters, mainly the foaming temperature and soaking time, as well as by using a double step depressurization. This peculiar depressurization protocol has been selected to obtain foams with a double-scale of pore sizes suitable as scaffolds for bone tissue engineering. Indeed, porous scaffolds with large and small pores have been found to provide a better substrate for cell growth and colonization [17].

2. Experimental

2.1. Materials

PCL with a molecular weight (Mn) of 80 kDa and ethyl lactate (EL) (photoresistant grade; purity ≥99.0 wt%) were purchased from Sigma-Aldrich (Madrid, Spain). Ethanol (96% v/v) and ethyl acetate (EA) were provided by Panreac (Barcelona, Spain). Two different kinds of HA particles were used as the inorganic filler for the preparation of the composite materials. A micrometric size HA powder, with a mean particle size of 10 μm, was synthesized as described in a previously reported work [18]. A commercially available nanometric size HA powder, with particle sizes lower than 200 nm and surface areas higher than 9.4 m^2/g, was provided by Sigma-Aldrich, Madrid, Spain. All reagents were used without further purification.

2.2. Preparation of PCL and PCL–HA composites powders

The polymer and the inorganic fillers were processed by a solution-based phase separation technique in order to prepare PCL–HA composite powders. First, a homogeneous suspension of EL containing a definite amount of HA particles was achieved by means of magnetic stirring (30 min) followed by sonication (30 min). Subsequently, the temperature of the suspension was increased up to 60 °C followed by the addition of 30 wt% of PCL, with respect to the EL, under magnetic stirring. The solution was maintained at these conditions overnight in order to achieve the complete dissolution of the polymer. Micrometric size particles of PCL–HA composites were achieved by a thermal induced phase separation process, according to the procedure described in [19]. In particular, the solution was cooled down to −15 °C for 3 h to induce gelation and it was further soaked in excess of water for 15 min under magnetic stirring. This step allowed the extraction of the EL and the consequent precipitation of the polymeric powder containing the HA particles. The obtained composite was subsequently washed twice with fresh water up to the complete removal of EL. Afterwards the material was dehydrated in ethanol before being dried at room temperature and ambient pressure. If compared to conventional melt blending procedures, this solution-based process is expected to reduce the amount of aggregated filler and to increase the dispersion in the polymeric matrix. By this method, PCL–HA composites were prepared containing 5 and 10 wt% of nominal concentration of nano and micrometer sized HA particles. The same approach was also carried out on pure PCL for comparison.

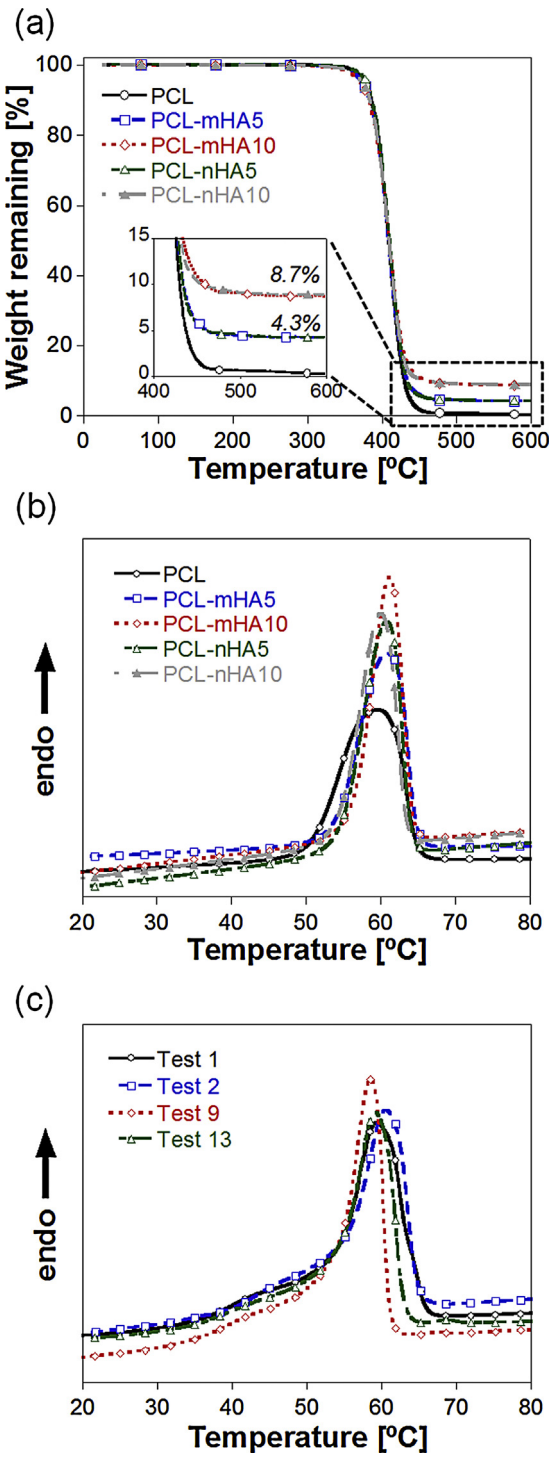

Fig. 1. (a) TGA and (b) DSC curves of the different materials before foaming experiments; (c) DSC curves of selected PCL foams.

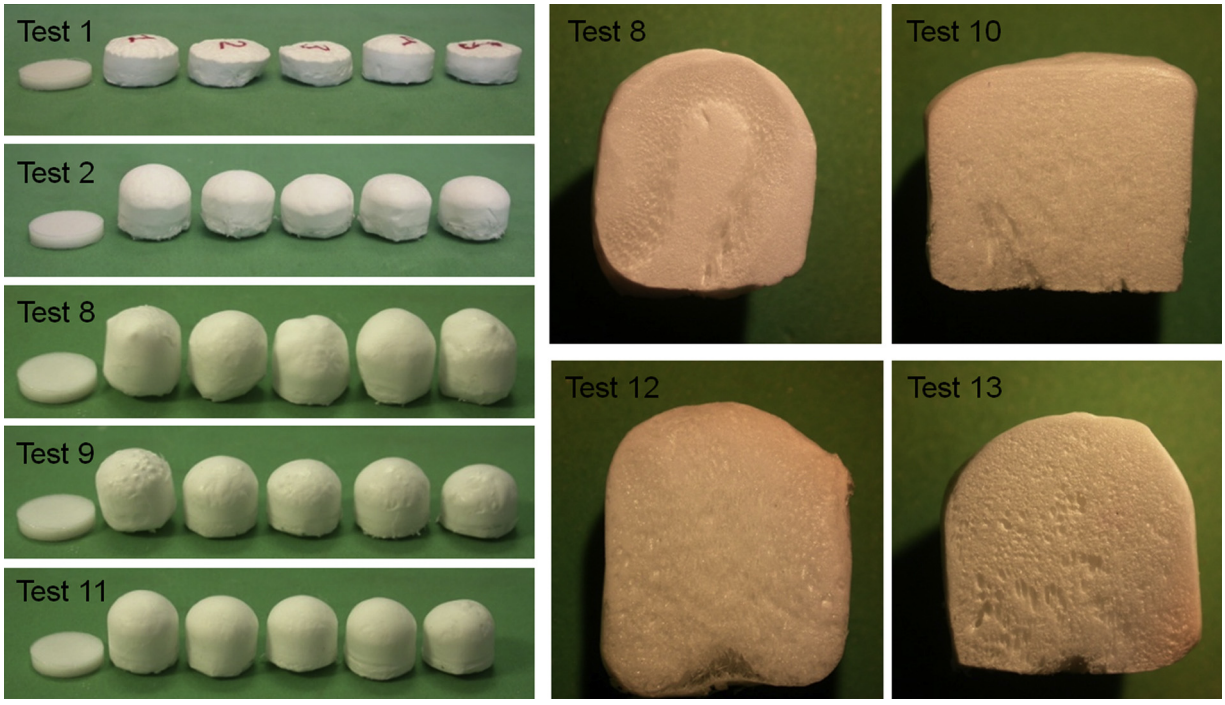

Fig. 2. Optical images of selected foams and cross-sections.

2.3. Foaming procedures

$ScCO_2$ foaming experiments were carried out on disc-shaped samples measuring 13 mm of diameter and 2 mm of thickness. The samples were prepared by the compaction of 0.3 g of PCL or PCL–HA composite powders at 3.7 MPa using a hydraulic press. Foaming experiments were carried out in a 114 mL high-pressure autoclave (TharDesign, Madrid, Spain). Samples were placed inside of the autoclave on the top of a metallic support to allow for the addition of a magnetic stirrer at the bottom of the vessel. This configuration is used to improve fluids mixing and to reduce the equilibrium time. The temperature was then raised up to the operating temperature, either 40 or 45 °C, and liquid CO_2 was pumped inside the vessel, by means of a high pressure pump (260 D, Lincoln, USA), up to 20 MPa to ensure the achievement of supercritical conditions. Samples were held at these conditions for different soaking times, either 1 h or 17 h, after which foaming was induced by quenching the pressure to ambient conditions. A two-step depressurization profile, characterized by a slow initial depressurization stage going to an intermediate pressure of 7 MPa, followed by a fast gas release to atmospheric pressure, was used to induce samples foaming and to control the final porous structure [20]. This was carried out by a pressure release system consisting of a ball valve connected to a discharge capillary [19]. The main advantage of using this setting is related to the possibility of simultaneously controlling both pressure quench

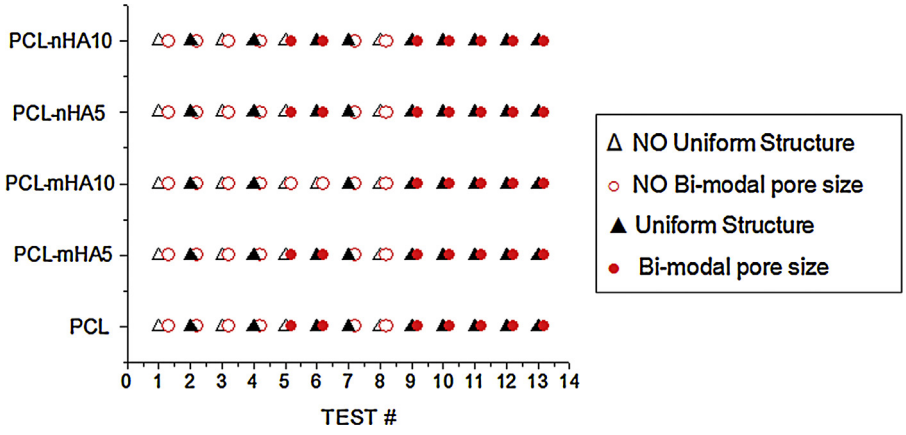

Fig. 3. Effect of operating conditions on the pore uniformity and pore structure of the foams.

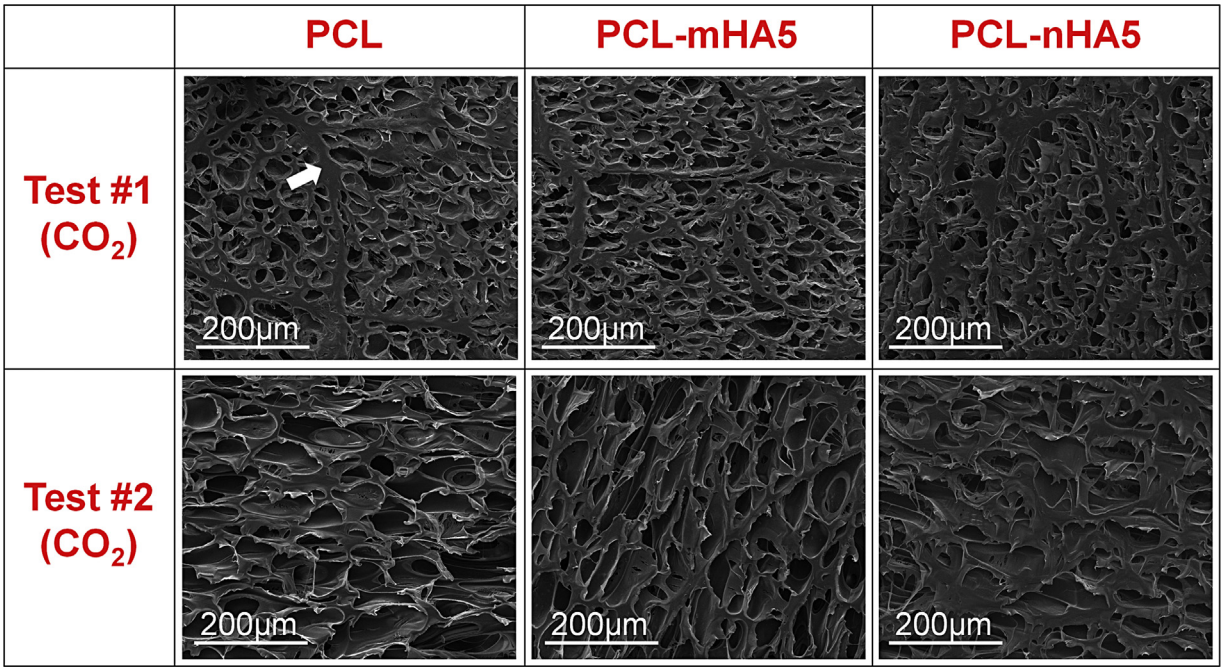

Fig. 4. Effect of composition and operating temperature on the morphology of selected foams prepared in Test 1 and 2.

profile and the overall time of depressurization by the opening/closing of the ball valve and by selecting discharge capillaries of appropriate length and diameter. In particular, after CO_2 solubilisation in the polymer, the ball valve was opened and the gas was released to a pressure of 7 MPa by using a slow discharge capillary. Subsequently, the ball valve was closed, the capillary substituted by a fast depressurization capillary and the pressure was quenched to the ambient by re-opening the ball valve. By considering that decreasing the depressurization rate reduces pore nucleation rate while promotes pore growth [19], this approach is expected to induce the formation of large pores in the first step of depressurization and small pores after the second depressurization step.

Additional foaming experiments were carried out by adding 500 μL of either EL or EA as plasticizers following two different protocols. In the first approach, the disc-shaped samples were prepared as described previously and 500 μL of plasticizer were added at the bottom of the high pressure vessel (named as route 1). Conversely, the second approach involved the preparation of a dough of powder (0.3 g) and 100 μL of plasticizer by manual mixing with a spatula (named as route 2). The mixtures were then compacted into disc-shaped samples with a hydraulic pressure of 15 MPa, suitable to avoid the diffusion of the plasticizer out of the powder, while achieving the desired geometry. By considering that the five compositions, namely PCL, PCL–mHA5, PCL–mHA10, PCL–nHA5 and PCL–nHA10, were processed at the same time during each test, the overall amount of plasticizer into the pressure vessel for each test was equal to 500 μL also in the case of dough samples. Consequently, the total mass of material with respect to the amount of plasticizer in the two routes was held constant. Immediately after preparation, the samples were processed using $scCO_2$ under different operating conditions. Table 1 summarizes the tests carried out were the number of each test refers to only one experiment in which all of the compositions were processed at the same time.

2.4. Characterization

Thermo-gravimetric (TGA-DTGA) analyses were carried out on PCL and PCL–HA composite powders to evaluate the thermal stability of the materials as a function of their composition and to assess the retained amount of inorganic filler with respect to the used nominal concentration during powder preparation. The experiments were carried out on a TGA STA 449 F1 Jupiter (NETZSCH, Selb, Germany) in the 30–600 °C temperature range at a rate of 10 °C/min under inert atmosphere. The HA loading for each composite was evaluated as the difference between the residues of the composites and pure PCL at 600 °C.

Differential scanning calorimetry (DSC) analyses were carried out on the PCL and PCL–HA composite powders, as well as on selected foams, in order to assess the effect of the composition and the processing parameters on the melting behaviour and the percentage of crystallinity of the samples. Samples were tested on a DSC8500 apparatus (Perkin Elmer, Massachusetts, USA) equipped with a liquid N_2 controller CRYOFILL. Samples were first equilibrated at 10 °C for 1 min and then heated up to 90 °C at a scanning rate of 10 °C/min under inert atmosphere. The melting range (ΔT_M), the melting peak temperature (T_M), the onset temperature (T_{ons}) and the crystallinity of the samples were determined from the analysis of the DSC curves.

The microstructure of the foams was assessed by optical and scanning electron microscopy (SEM) analysis. For SEM analysis, the samples were cross-sectioned by a razor blade at room temperature, gold sputtered and analyzed by a SEM instrument (QUANTA 200F FEG-ESEM, FEI, The Netherlands).

The porosity of the foams was assessed by using the following equation:

$$\text{porosity} = \left(1 - \frac{\rho_F}{\rho_B}\right) \times 100$$

where ρ_F is the density of the foams, as determined from mass and volume measurements, while ρ_B is the density of the bulk

material as determined from the theoretical density of PCL and HA and correcting the fraction of HA particles as assessed from TGA tests values. The mass of the samples was measured using a high accuracy balance (Sartorius Balance (YDK01), while the volume was determined by a displacement method (ASTM D1622-03).

The mean pore size of the foams was evaluated by image (Image J®) analysis. About one hundred pores for each sample were analyzed by using the "particle analysis" tools of the Image J® software package, which enabled to assess the area of each pore. The pore diameter was then calculated with the hypothesis of spherical shape pores and by correcting the as-obtained values by a $4/\pi$ factor, according to the ASTM D3576.

The pore density of the foamed samples was calculated by using the following equation [20]:

$$\text{pore density} = \left(\frac{n}{A}\right)^{3/2} \times \frac{\rho_B}{\rho_F}$$

where n is the number of pores and A is the area of the SEM micrograph selected for analysis.

3. Results

3.1. Thermal properties of the materials

The thermal behaviour of the samples is presented in Fig. 1. From TGA curves, the retained HA amount in the composites may be assessed by comparing the weight loss values of neat PCL and its composites with HA at the temperature of 600 °C. A loading amount of inorganic filler equal to 86–87 wt% of its nominal concentration was estimated for all composites (Fig. 1a). Fig. 1b and c shows the DSC scans of the PCL and PCL–HA composite materials before and after foaming. Melting peak values together with the melting intervals and samples crystallinity are listed in Table 2. The melting temperature (T_M) of the samples was not substantially affected by either the amount or nature of the added inorganic filler. T_M values between 60 and 61 °C were observed for non foamed powders. A slight decrease in the T_M values was observed after foaming. The percentage of crystallinity was affected by foaming, since a reduction of about 30% in crystallinity was observed in the processed samples.

3.2. Foaming processes

Fig. 2 shows the optical images of five selected series of samples after foaming. From four different tests, the change in volume and the general features of cross section is also shown in Fig. 2. The characteristics of the obtained samples indicate that the achievement of uniform foaming in the entire cross-section of the samples is observed when the materials are processed at 45 °C during 17 h in presence of a plasticizer. The amount of inorganic filler produces slight differences in the volume changes in each series of composites. The effects of the operating conditions on the uniformity of the cross-section of the foams and the development of a bi-modal pore size distribution are shown in Fig. 3. Obviously, a temperature of 45 °C is necessary to achieve uniformly foamed samples for all of the compositions, while the development of a bi-modal pore size structure requires the largest saturation time.

3.2.1. Effect of temperature on the foaming process

The effect of temperature on foam morphology is shown in Fig. 4 for PCL and 5%HA-PCL (nano or micro) composites processed at 40 °C and 45 °C. At the lowest temperature of foaming, a microstructure characterized by clearly confined sections of pores was observed, indicating that no complete melting occurred during the soaking period (Fig. 4 Test#1). When the samples were processed at 45 °C, porous homogeneous microstructures were obtained (Fig. 4 Test#2).

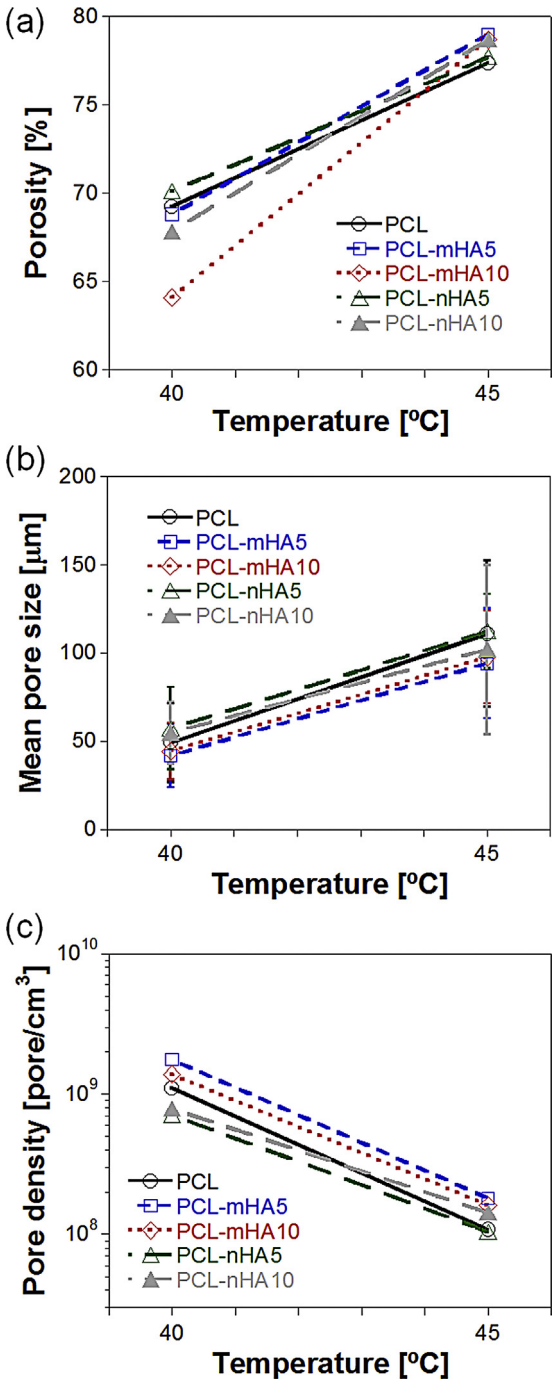

Fig. 5. Effect of composition and operating temperature on (a) porosity, (b) mean pore size and (c) pore density of PCL and PCL–HA composite foams prepared in Test 1 and 2. The continuous and dotted lines are for eye guidance purpose.

Fig. 5 shows the effect of the foaming temperature on porosity, mean pore size and pore density on the series of samples obtained from Test #1 and Test #2. An increase in porosity and in mean pore size values was observed when the temperature increased from 40 °C up to 45 °C. The porosity and mean pore size values increased by 13% and 100%, respectively. However, a reduction of a logarithmic order was observed in the pore density for the same interval of temperature.

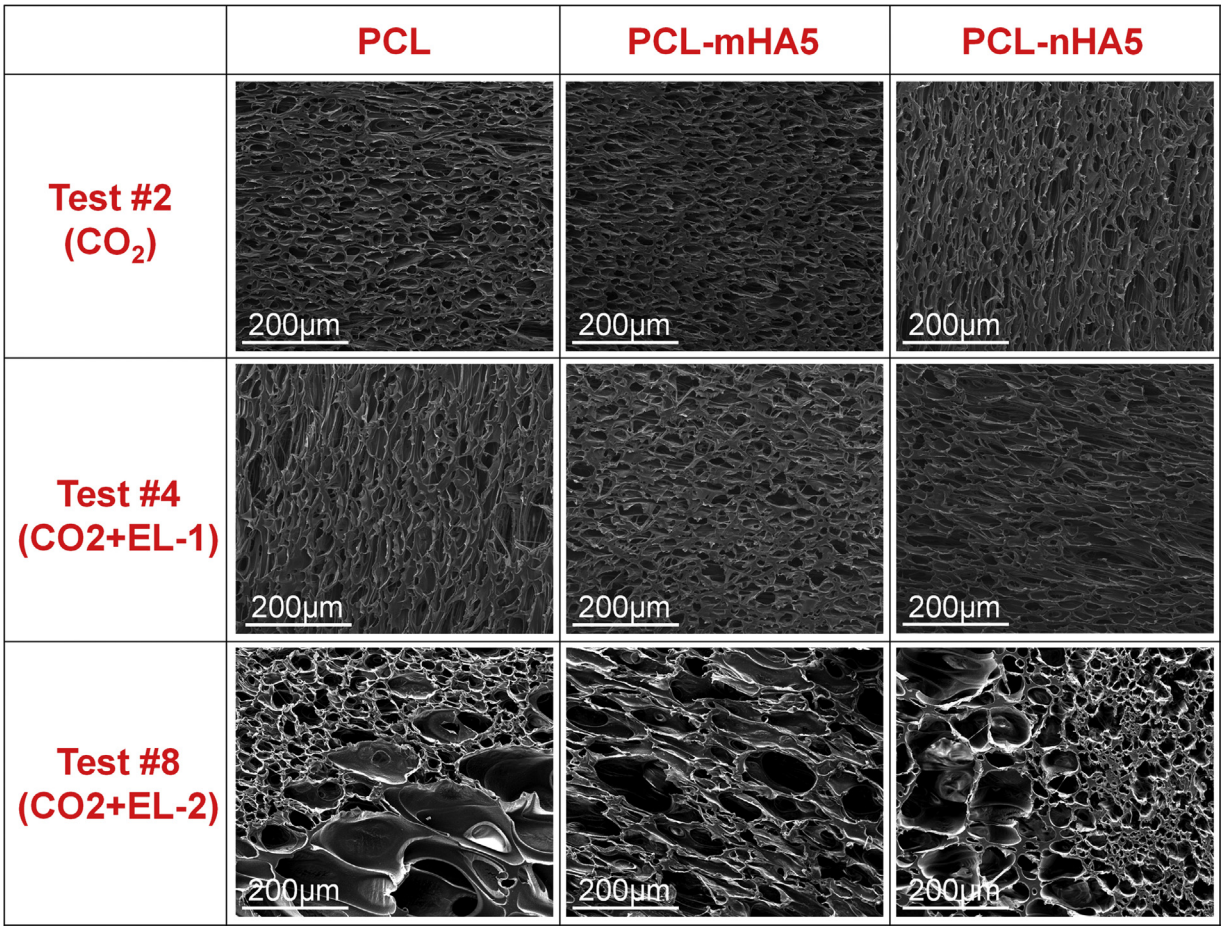

Fig. 6. Effect of composition and EL addition on the morphology of selected foams prepared in Test 2, 4 and 8.

No relevant variations in these microstructural parameters by effect of composition and nature of the inorganic fillers were observed on the characteristics of the foams.

3.2.2. Effect of EL on the foaming process

Fig. 6 shows the microstructure of the samples after foaming at 45 °C with EL incorporated by the two different routes described above. Heterogeneous microstructures were observed in samples compacted from a dough following route 2 (Test #8). However, more homogeneous pore distribution and mean pore size values were measured on processed samples applying route 1 of incorporation of EL (Test #4). These parameters were slightly increased with respect to those without incorporated EL (Test#2).

Fig. 7 shows the microstructural characteristics of foamed samples at two temperatures, where the effect of the route of incorporation of EL is shown. At 40 °C, the incorporation of EL into the samples (EL-2, test#7) produces an increase in the porosity compared to the incorporation of EL by route 1 (EL-1, test#3). The inorganic filler content does not seem to be relevant on the obtained porosity values. In general, the increase in the mean pore size in EL-2 is associated with a reduction in the pore density values. At 45 °C, the incorporation of EL by route 1 (EL-1, test#4) produces a significant increase in the porosity with respect to the foamed samples without EL (test#2). The EL-2 incorporation resulted in higher porosity values and inhomogeneous microstructures (Fig. 6). The HA content slightly affected the final value of porosity. Higher contents of inorganic filler results in lower porosity values (test #8). The mean pore size and pore density values in foamed samples following the EL-2 process (test #8) could not be evaluated due to inhomogeneities in the microstructures.

Figs. 8 and 9 show the obtained results of the characterization of samples processed during 17 h of saturation time at 45 °C and with added EL. SEM images show materials with homogeneous microstructures from tests #9, #10 and #12. A bi-modal pore size distribution was observed in all samples of both series EL-1 and EL-2. In general, the increase in porosity values was similar to that observed for the series processed during 1 h. However, the resulting microstructures presented an improved bi-modal distribution of pore sizes with respect to the samples obtained by the foaming processes with only 1 h of saturation time. By adding EL, forming a dough with the inorganic powder (EL-2), the generation of macropores (250–300 µm) is favoured.

3.2.3. Effect of EA on the foaming process

Fig. 10 shows the effect of process temperature on sample microstructures after foaming by adding EA introduced by route 2 (EA-2). It can be seen that at 45 °C the resulting microstructures were more homogeneous than at 40 °C, except for the sample containing 10 wt% mHA (not shown). The effect of the EA addition method is shown on the microstructures of the samples in Fig. 11. For foamed samples using the EA-2 method, low and high magnification SEM images are shown in Fig. 11, evidencing the formation of macropores with a mean pore diameter greater than in samples foamed by the EA-1 route.

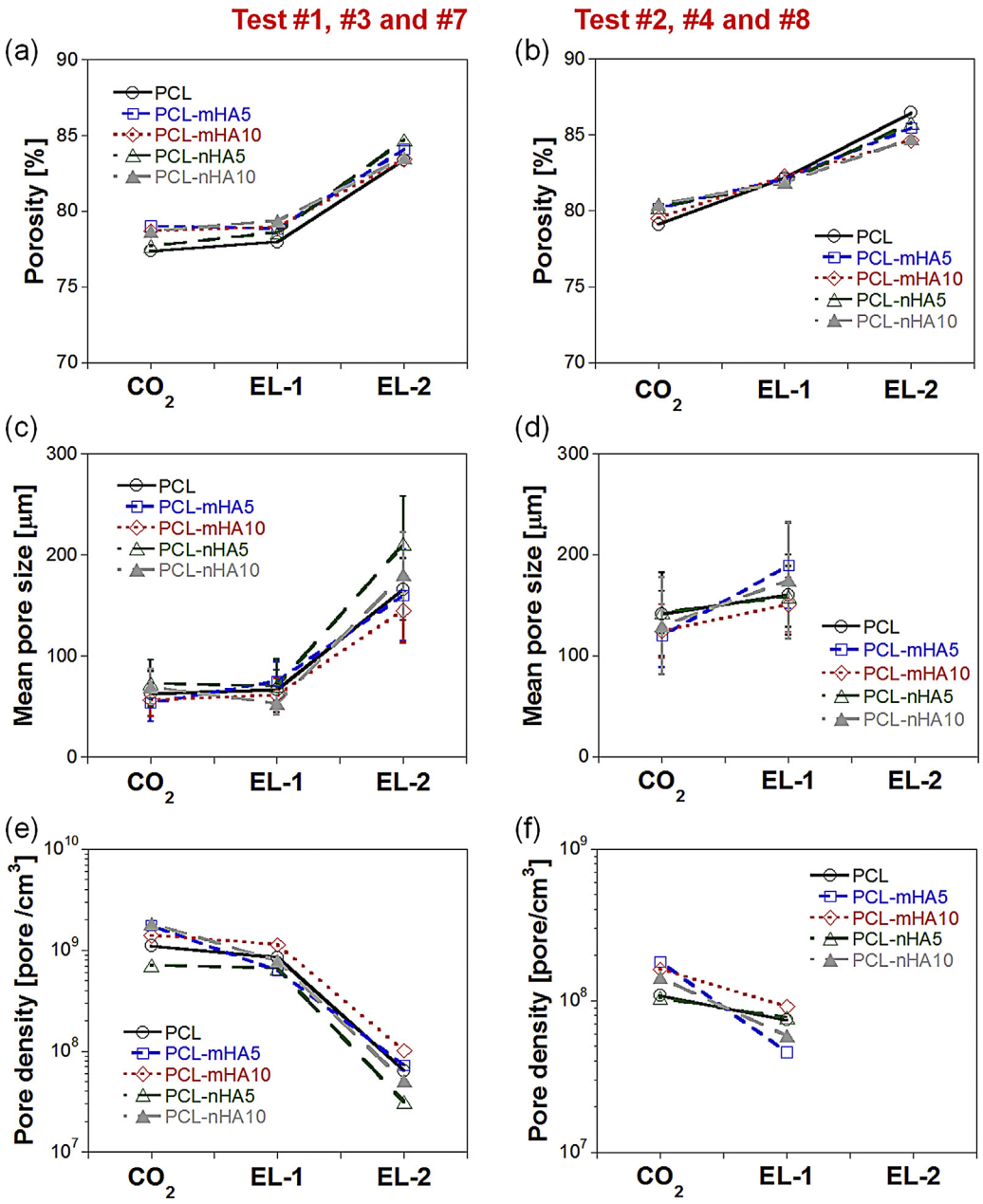

Fig. 7. Effect of composition and EL addition on (a and b) porosity, (c and d) mean pore size and (e and f) pore density of PCL and PCL–HA composite foams prepared at (a, c and e) 40 °C and (b, d and f) 45 °C.

The porosity and the mean pore sizes of small and large pores for samples foamed with EA (Fig. 12) are in accordance with the observed microstructures.

4. Discussion

Foaming of biodegradable and biocompatible polymers and composites by means of $scCO_2$ enables the production of three dimensional porous scaffolds whose properties, mainly overall porosity, pore size distribution and pore interconnectivity, can be fine tuned by the appropriate selection of the processing conditions [9–11,14]. The high sorption of $scCO_2$ within a wide range of polymeric biomaterials, such as biodegradable polyesters, reduces their viscosity by decreasing both the glass transition and melting temperatures [21,22]. This peculiar behavior of $scCO_2$ opens unique opportunities in the field of tissue engineering, as it allows preparing bioactive porous scaffolds and controlled drug delivery platforms in a safe and clean approach [14,23]. However, results reported in literature up to date suggest that working with highly crystalline polymers and their composites at temperatures below the melting value makes the foaming difficult to control, because of the complex interaction established between sc-CO_2 and the crystalline structure of the polymer [24].

In development of polymeric-ceramic composites, a great challenge is to achieve an appropriate blending of the polymeric and inorganic components for producing a multi-phase material with improved properties. This goal is of great importance especially in the case of nano-composites, due to the tendency of the nanoparticles to agglomerate. In this work, the thermally

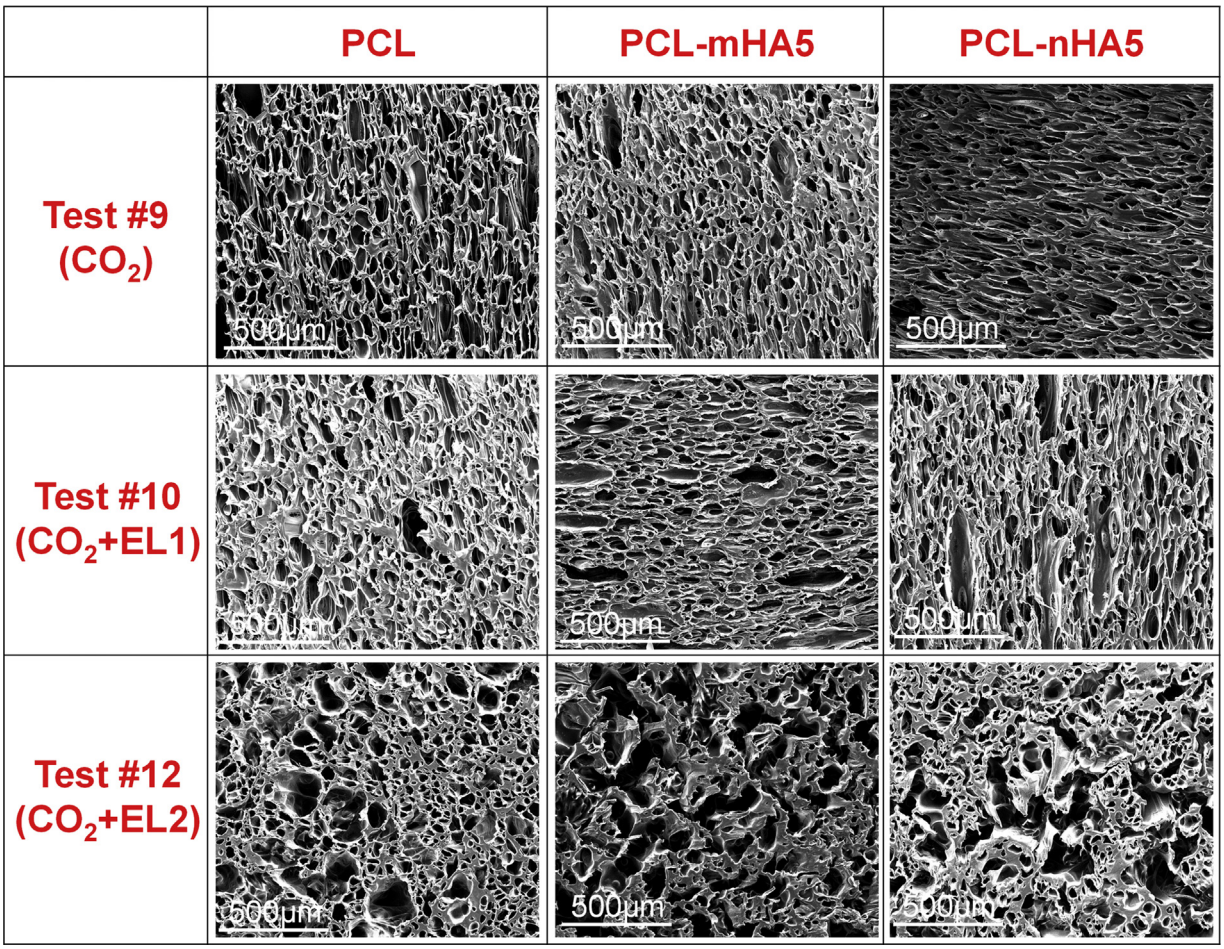

Fig. 8. Effect of composition and EL addition on the morphology of selected foams prepared in Test 9, 10 and 12.

induced phase separation route developed to prepare PCL–HA nano- and micro-composites [19] allows a high filler loading efficiency and dispersion inside the polymeric matrix. By considering that pure PCL is completely degraded in the range of 300–500 °C (Fig. 1a), it is considered appropriate to estimate the inorganic filler amount loaded in the composite by measuring the residual weight at 600 °C. For all of the PCL–HA composites prepared in this work, the percentage of inorganic filler retention was higher than 85%, clearly indicating the consistency of the used preparation method.

The presence of inorganic fillers slightly increased the T_M and crystalline fraction of the composites (Fig. 1b). This effect was ascribed to the heterogeneous crystallization of the polymer that occurs in the composites. Indeed, the HA filler can act as a center of precipitation of PCL during the solution-based phase separation process, thus, increasing the polymer nucleation. Conversely, during foaming with sc-CO_2, the HA particles can act as obstacles for the crystallization process from melted PCL, and a decrease in the percentage of crystallinity in the composites after foaming is observed (Fig. 1c).

In this work, PCL and PCL–HA composite foams are prepared by a scCO_2 foaming process carried out at temperatures below the PCL melting, while the characteristics of the pore structure of the foams are controlled by the appropriate selection of the operating parameters. It is important to point out that, once scCO_2 solubilization in the polymer is completed, a double depressurization step is used to induce samples foaming. As reported in a previous work, this particular pressure quench profile is selected to induce the formation of a porous structure characterized by a double distribution of pore sizes [11,20]. Indeed, porous scaffolds provided of a multi-scaled pore size distribution have been reported to enhance the biological response of PCL scaffolds for bone tissue engineering [17]. Therefore, achieving this goal for the composites described in this work is important for their use in tissue engineering applications.

As shown in Fig. 2 all of the operating conditions selected for foaming PCL and its composites with HA particles result in foamed samples with microporous structures. However, visual observation of the samples clearly indicates that foaming decreases slightly with the increase of filler content, while an operating temperature of 45 °C results in enhanced foaming for all of the tested compositions (compare tests #1 and #2). As the most important result, it was found that whether or not a uniform and highly porous structure was obtained depends on both, sample preparation and soaking time. For instance, by comparing the optical images of the cross section of the PCL samples of Test #8 and #12 reported in Fig. 2, it is clear that 1 h of soaking time is not sufficient to achieve PCL foams with uniform morphology starting from a PCL–EL dough. As a direct consequence, we observed an inner region of small pores surrounded by an outer region of large pores. This effect is ascribable to the procedure used for the preparation of the samples as well as to the time required to scCO_2 and EL to be homogeneously distributed inside the polymeric matrix. In particular, it is possible that the manual mixing of powder and plasticizer used to prepare

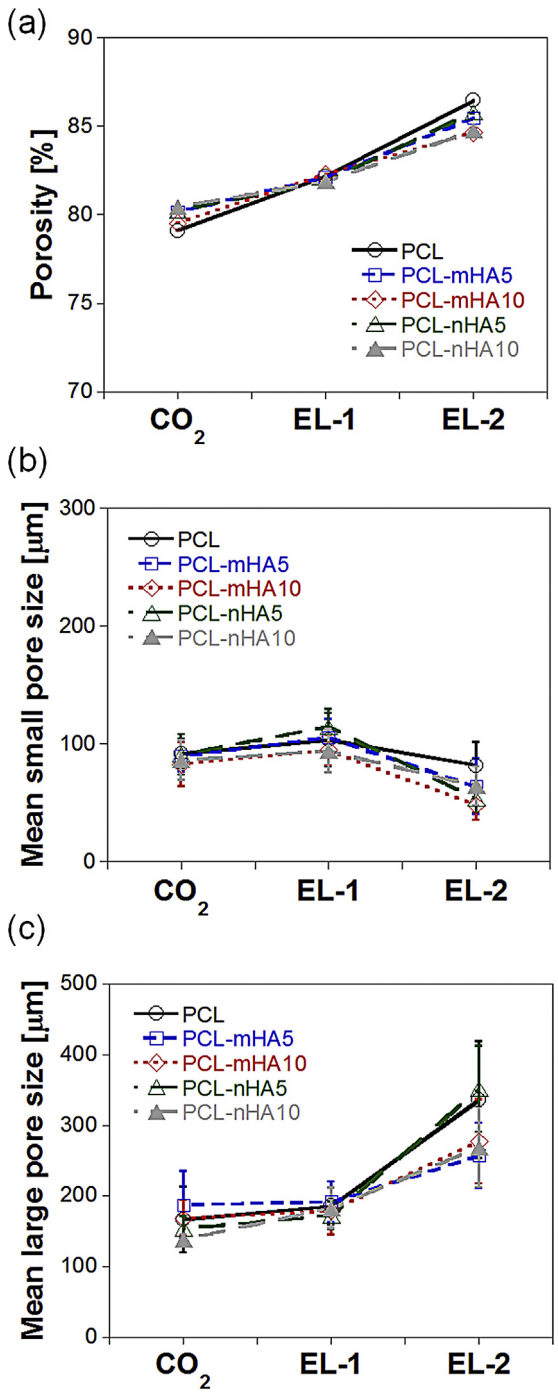

Fig. 9. Effect of composition and EL addition on (a) porosity, (b) mean small pore size and (c) mean large pore size of PCL and PCL–HA composite foams prepared at 45 °C.

the dough, followed by its compaction, cannot ensure an optimal distribution of the components. Furthermore, the sCO_2 processing of the dough for a short period of time was likely unable to produce a homogeneous distribution of $scCO_2$ and EL inside the samples. Conversely, increasing the soaking time up to 17 h allows for the blowing agent to mix uniformly inside the polymeric matrix and, consequently, results in PCL and PCL–HA composite foams with uniform morphology. These considerations are also corroborated by the SEM analysis of the cross section of the samples reported in Figs. 6 and 8.

Optimizing the operating temperature is also of great importance in the foaming of semi-crystalline polymers at temperatures lower than the melting range. Based on the room temperature compaction of the powder materials, it is possible to evaluate polymer melting by the SEM analysis of the cross section of the foams. Increasing the operating temperature from 40 to 45 °C facilitates polymer melting when the material is contacted with $scCO_2$ at 20 MPa, as indicated by the disappearing fusion lines between adjacent particles shown in Fig. 4. Furthermore, enhanced foaming was achieved at the highest temperature investigated. These effects are in agreement with literature data, related to the melting behavior of PCL under high pressure of CO_2 [10,11,22].

Compared to the melting temperature at atmospheric pressure, there is a dramatic reduction in the melting temperature observed under pressure. The variation of T_M with CO_2 pressure has been determined from high pressure DSC data and is reported in Ref. [14]. For instance, the melting occurs already at 33 °C at 10 MPa. The ability of PCL to melt in the range of 33–40 °C when being contacted with $scCO_2$ has also been corroborated by visual monitoring the sample behaviour over soaking time [10] and by indirect observation of foam morphology [11]. The results of this work are in agreement with literature data, even if though it was found that a slightly higher temperature of 45 °C provides the most convenient melting and foaming behavior of PCL and its composites with HA. Furthermore, as shown in Figs. 2 and 8, by increasing the soaking time up to 17 h, while keeping the temperature constant at 40 °C, PCL melting and foaming is enhanced. This effect suggests that $scCO_2$ soaking conditions, mainly temperature and time, should be adjusted depending on polymer properties and sample geometry, as well as on the required applications.

The efficiency of combining $scCO_2$ with EL and EA as plasticizers is demonstrated in this work. The samples prepared by using binary mixtures as foaming agents contain a morphology that is more homogeneous with a higher porosity and larger pores sizes than using pure $scCO_2$ (Figs. 6–9). This effect has previously been shown by the use of acetone [25] and ethanol [26]. In this work, we further improved this approach by comparing the effect of using EL and EA as plasticizers for $scCO_2$ foaming of PCL and PCL–HA nano- and microcomposites, where different methods of adding these plasticisers are evaluated. These solvents are miscible with CO_2 at high pressure [20,27] and are obtained *via* the esterification of ethanol, respectively, with lactic and acetic acid, both generated from biomass. Therefore, they represent good alternatives to the traditional organic plasticizers of fossil origin for polymer processing.

Achieving a multi-scaled pore structure is of great importance for applications related to tissue engineering, were scaffolds with pores larger than 100 μm are necessaries to allow for the three dimensional adhesion and colonization with cells, as well as for new tissue development *in vitro* and *in vivo* [17]. The use of a double step of depressurization during the foaming process has been reported to be an efficient approach to achieve this goal avoiding the use of additional compounds or processes [11]. As shown in this work, using this experimental setup the resulting pore structure of PCL and PCL–HA foams is strongly dependent on the selection of the plasticizer, as well as on the other operating parameters, namely samples preparation, foaming temperature and soaking time. In particular, the best results are achieved when the EA is mixed with PCL and its composites to form compacted doughs and these samples are maintained in contact with $scCO_2$ for 17 h (Fig. 11). Indeed, these samples have 80% overall porosity values and the double scale pore structure evidences small pores in the 60–80 μm range coupled to larger pores in the 250–350 μm range (Fig. 12).

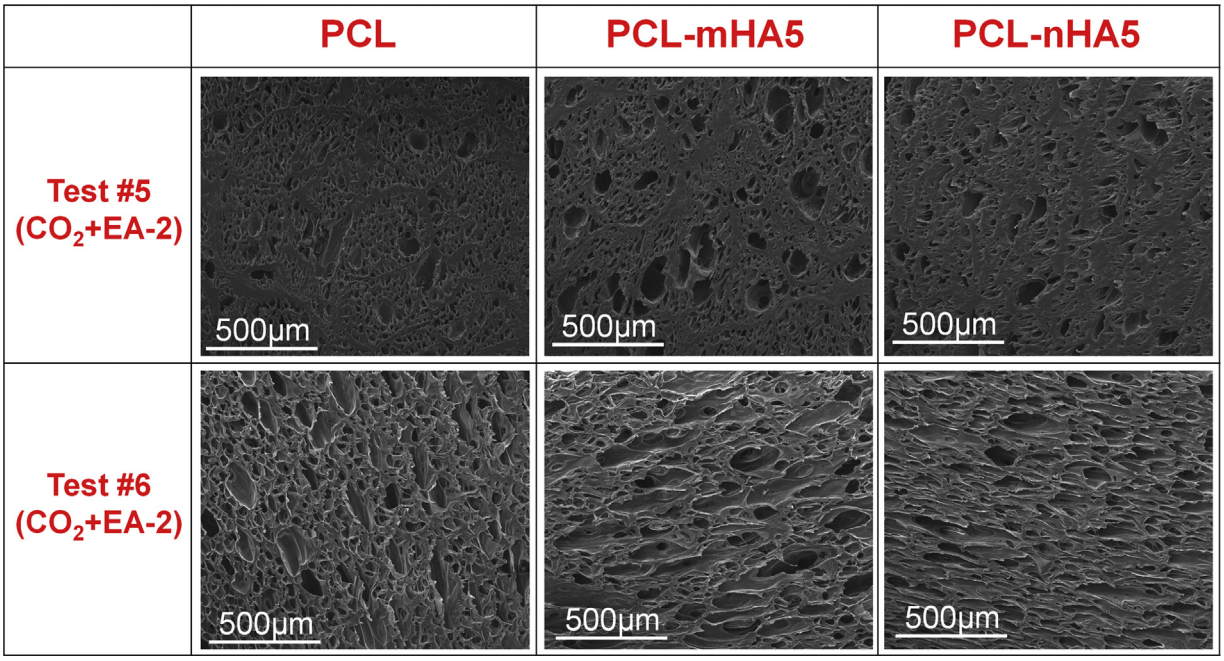

Fig. 10. Effect of composition and operating temperature on the morphology of foams prepared by means of the EA-2 process.

The used methodologies can be represented as shown Fig. 3. The more interesting effect was obtained when the plasticizer was introduced by forming a compacted dough and maintained in contact with $scCO_2$ during a large period of time. The concentration of plasticizer into the material differs according to the used method. Also, the generated interaction between the plasticizer and the composed matrix play a relevant role. In particular, when the plasticizer was used during the foaming tests, EA provided better results if compared to EL, especially in terms of foam morphology and the development of a more homogeneous bi-modal porous structure. By considering the Hildebrand solubility parameters of EA, EL and PCL, which are 19 [28], 21.3 [29] and 19.7 [30], respectively, it is possible to determine that EA is a better solvent for PCL than EL. This consideration is supported by the experimental evidence that the plasticization of PCL powder when mixed with the plasticizer for preparing the dough is enhanced in the case of EA if compared to EL. Concomitantly, EA, being less polar than EL (their relative dielectric permittivity at room temperature are 6.08 and 15.7, respectively) [31,32], is thus more chemically affine to $scCO_2$ and can promote the formation of the binary mixture. This consideration is supported by literature investigations on phase diagrams of $scCO_2$ and used plasticizers, which have

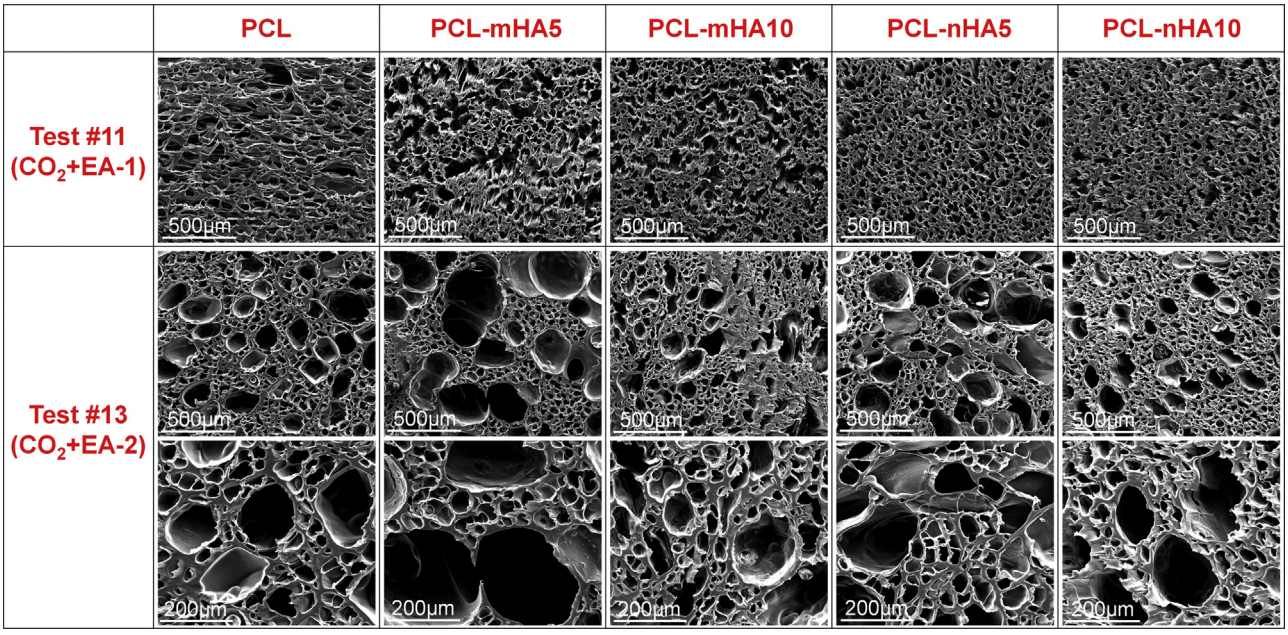

Fig. 11. Effect of composition and EA addition on the morphology of foams prepared at 45 °C and 17 h of saturation time.

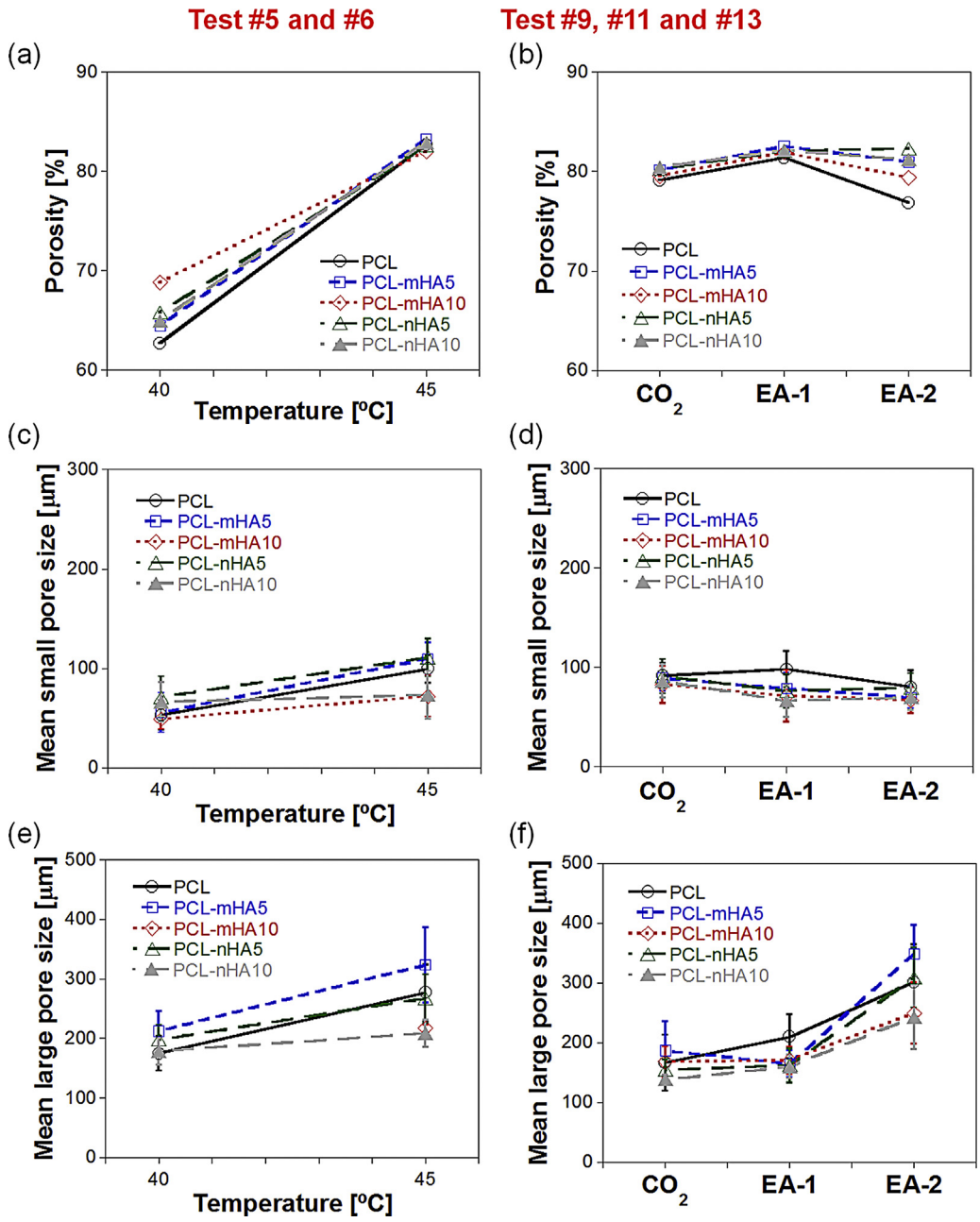

Fig. 12. Effect of composition, operating temperature and EA addition on the (a and b) porosity, (c and d) mean small pore size and (e and f) mean large pore size of PCL and PCL–HA composite foams. (a, c and e) tests #5 and #6, (b, d and f) tests #9, #11 and #13.

evidenced the enhanced solubility of $scCO_2$ into EA rather than EL [33,34].

5. Conclusions

In this work, low temperature foaming of PCL and PCL–HA composites by means of $scCO_2$ and binary mixtures of $scCO_2$ and EL or EA as plasticizers is reported. Obtained results demonstrated that, by the appropriate control of the processing parameters, namely the route of incorporation of plasticizer, blowing agent mixture composition, operating temperature and soaking time, it was possible to fabricate PCL and PCL–HA composite foams with homogeneous pore morphology and tailored pore structure features. In particular, the addition of EL and EA to $scCO_2$ enhanced the plasticization ability of the blowing mixture, while this effect was more evident at the highest temperature and soaking time investigated. As a direct consequence, homogeneous foams with porosities up to 87% and a double scale pore size distribution were achieved, being potential bioactive materials for scaffolds in tissue engineering applications.

Acknowledgements

Aurelio Salerno acknowledges the CSIC for the financial support through a JAE-DOC contract cofinanced by the FSE. The authors also acknowledge the financial support of the Ministerio de Economía y Competitividad through the research project BIOREG (MAT2012-35161) and the European Union for the founded project

EULA-NETCERMAT (PIRSES-GA-2011-295197). Additional support has been provided by the Generalitat of Catalonia under project 2014SGR-377 and by the National Research Council PIP1851 (CONICET, Argentina).

References

[1] Arun R. Shrivats, Michael C. McDermott, Jeffrey O. Hollinger, Bone tissue engineering: state of the union, Drug Discovery Today 19 (6) (2014) 781–786.
[2] Yi Li, Zhi-gang Wu, Xiao-kang Li, Zheng Guo, Su-hua Wu, Yong-quan Zhang, Lei Shi, Swee-hin Teoh, Yu-chun Liu, Zhi-yong Zhang, A polycaprolactone-tricalcium phosphate composite scaffold as an autograft-free spinal fusion cage in a sheep model, Biomaterials 35 (22) (2014) 5647–5659.
[3] Kyung-A. Kwak, Young-Hee Kim, Minsung Kim, Byong-Taek Lee, Ho-Yeon Song, Bio-functionalization of polycaprolactone infiltrated BCP scaffold with silicon and fibronectin enhances osteoblast activity in vitro, Applied Surface Science 279 (15) (2013) 13–22.
[4] Lauren Shor, Selçuk Güçeri, Xuejun Wen, Milind Gandhi, Wei Sun, Fabrication of three-dimensional polycaprolactone/hydroxyapatite tissue scaffolds and osteoblast-scaffold interactions in vitro, Biomaterials 28 (35) (2007) 5291–5297.
[5] Seyed-Iman Roohani-Esfahani, Saied Nouri-Khorasani, Zufu Lu, Richard Appleyard, Hala Zreiqat, The influence hydroxyapatite nanoparticle shape and size on the properties of biphasic calcium phosphate scaffolds coated with hydroxyapatite-PCL composites, Biomaterials 31 (21) (2010) 5498–5509.
[6] N. Johari, M.H. Fathi, M.A. Golozar, Fabrication, characterization and evaluation of the mechanical properties of poly (ε-caprolactone)/nano-fluoridated hydroxyapatite scaffold for bone tissue engineering, Composites, B: Engineering 43 (3) (2012) 1671–1675.
[7] Fangfang Sun, Hongjian Zhou, Jaebeom Lee, Various preparation methods of highly porous hydroxyapatite/polymer nanoscale biocomposites for bone regeneration, Acta Biomaterialia 7 (11) (2011) 3813–3828.
[8] M. Sauceau, J. Fages, A. Common, C. Nikitine, E. Rodier, New challenges in polymer foaming: a review of extrusion processes assisted by supercritical carbon dioxide, Progress in Polymer Science 36 (6) (2011) 749–766.
[9] M. Karimi, M. Heuchel, T. Weiggel, M. Schossig, D. Hofmann, A. Lendlein, Formation and size distribution of pores in poly(ε-caprolactone) foams prepared by pressure quenching using supercritical CO_2, J. Supercritical Fluids 61 (2012) 175–190.
[10] M.A. Fanovich, P. Jaeger, Sorption and diffusion of compressed carbon dioxide in polycaprolactone for the development of porous scaffolds, Materials Science and Engineering C 32 (2012) 961–968.
[11] A. Salerno, E. Di Maio, S. Iannace, P.A. Netti, Solid-state supercritical CO_2 foaming of PCL and PCL–HA nano-composite: effect of composition, thermal history and foaming process on foam pore structure, J. Supercritical Fluids 58 (1) (2011) 158–167.
[12] A. Salerno, S. Iannace, P.A. Netti, Graded biomimetic osteochondral scaffold prepared via CO_2 foaming and micronized NaCl leaching, Materials Letters 82 (1) (2012) 137–140.
[13] A. Salerno, S. Zeppetelli, E. Di Maio, S. Iannace, P.A. Netti, Novel 3D porous multiphase composite scaffolds based on PCL, thermoplastic zein and ha prepared via supercritical CO_2 foaming for bone regeneration, Composites Science and Technology 70 (13) (2010) 1838–1846 (15).
[14] M.A. Fanovich, J. Ivanovic, D. Misic, M.V. Alvarez, P. Jaeger, I. Zizovic, R. Eggers, Development of polycaprolactone scaffold with antibacterial activity by an integrated supercritical extraction and impregnation process, J. Supercritical Fluids 78 (2013) 42–53.
[15] E. Markočič, M. Škerget, Ž. Knez, Solubility and diffusivity of CO_2 in poly(l-lactide)–hydroxyapatite and poly(d,l-lactide-co-glycolide)–hydroxyapatite composite biomaterials, J. Supercritical Fluids 55 (3) (2011) 1046–1051.
[16] I. Tsivintzelis, E. Pavlidou, C. Panayiotou, Biodegradable polymer foams prepared with supercritical CO_2–ethanol mixtures as blowing agents, J. Supercritical Fluids 42 (2) (2007) 265–272.
[17] A. Salerno, D. Guarnieri, M. Iannone, S. Zeppetelli, P.A. Netti, Effect of micro- and macroporosity of bone tissue three-dimensional-poly(ε-caprolactone) scaffold on human mesenchymal stem cells invasion, proliferation, and differentiation in vitro, Tissue Engineering, A 16 (2010) 2661–2673.
[18] M.A. Giardina, M.A. Fanovich, Synthesis of nanocrystalline hydroxyapatite from $Ca(OH)_2$ and H_3PO_4 assisted by ultrasonic irradiation, Ceramics International 36 (2010) 1961–1969.
[19] A. Salerno, C. Domingo, A novel bio-safe phase separation process for preparing open-pore biodegradable polycaprolactone microparticles, Materials Science and Engineering C 42 (2014) 102–110.
[20] A. Salerno, U. Clerici, C. Domingo, Solid-state foaming of biodegradable polyesters by means of supercritical CO_2/ethyl lactate mixtures: Towards designing advanced materials by means of sustainable processes, European Polymer J. 51 (2014) 1–11.
[21] R.B. Yoganathan, R. Mammuccari, N.R. Foster, Dense gas processing of polymers, Polymer Reviews 50 (2014) 144–177.
[22] Z. Lian, S.A. Epstein, C.W. Blenk, A.D. Shine, Carbon dioxide-induced melting point depression of biodegradable semicrystalline polymers, J. Supercritical Fluids 39 (2006) 107–117.
[23] M. Bhamidipati, A.M. Scurto, M.S. Detamore, The future of carbon dioxide for polymer processing in tissue engineering, Tissue Engineering, B 19 (2013) 221–232.
[24] C. Gualandi, L.J. White, L. Chen, R.A. Gross, K.M. Shakesheff, S.M. Howdle, M. Scandola, Scaffold for tissue engineering fabricated by non-isothermal supercritical carbon dioxide foaming of a highly crystalline polyester, Acta Biomaterialia 6 (2010) 130–136.
[25] E. Kiran, Foaming strategies for bioabsorbable polymers in supercritical fluid mixtures. Part I. Miscibility and foaming of poly(l-lactic acid) in carbon dioxide + acetone binary fluid mixtures, J. Supercritical Fluids 54 (2010) 296–307.
[26] I. Tsivintzelis, E. Pavlidou, C. Panayiotou, Biodegradable polymer foams prepared with supercritical CO_2-ethanol mixtures as blowing agents, J. Supercritical Fluids 42 (2007) 265–272.
[27] N. Falco, E. Kiran, Volumetric properties of ethyl acetate + carbon dioxide binary fluid mixtures at high pressures, J. Supercritical Fluids 61 (2012) 9–24.
[28] R. Auras, B. Harte, S. Selke, Sorption of ethyl acetate and d-limonene in poly(lactide) polymers, J. Science of Food and Agriculture 86 (2006) 648–656.
[29] C.S.M. Pereira, V.M.T.M. Silva, A.E. Rodrigues, Ethyl lactate as a solvent: properties, applications and production processes–a review, Green Chemistry 13 (2011) 2658–2671.
[30] C. Bordes, V. Fréville, E. Ruffin, P. Marote, J.Y. Gauvrit, S. Briançon, P. Lantéri, Determination of poly(ε-caprolactone) solubility parameters: application to solvent substitution in a microencapsulation process, International J. Pharmaceutics 383 (2010) 236–243.
[31] J.A. Dean, Lange's Handbook of Chemistry, 15th ed., McGraw-Hill, New York City, NY, USA, 1998.
[32] S. Aparicio, R. Alcalde, The green solvent ethyl lactate: an experimental and theoretical characterization, Green Chemistry 11 (2009) 65–78.
[33] Y. Tian, H. Zhu, Y. Xue, Z. Liu, L. Yin, Vapor–liquid equilibria of the carbon dioxide + ethyl propanoate and carbon dioxide + ethyl acetate systems at pressure from 2.96 MPa to 11.79 MPa and temperature from 313 K to 393 K, J. Chemical and Engineering Data 49 (2004) 1554–1559.
[34] D.W. Cho, M.S. Shin, J. Shin, W. Bae, H. Kim, High-pressure phase behavior of methyl lactate and ethyl lactate in supercritical carbon dioxide, J. Chemical and Engineering Data 56 (2011) 3561–3566.